

Transition to helical RFP state and associated change in magnetic stochasticity in a low-aspect-ratio RFP

S.Masamune

Kyoto Institute of Technology, Kyoto 606-8585, Japan

A.Sanpei, R.Ikezoe, T. Onchi, K.Oki, T.Yamashita, Y.Konishi, M.Nakamura, M.Sugihara, A.Higashi, H.Motoi, H. Himura, N.Nishino¹⁾, R.Paccagnella²⁾, A.Ejiri³⁾, H.Koguchi⁴⁾

Kyoto Institute of technology, Kyoto, Japan

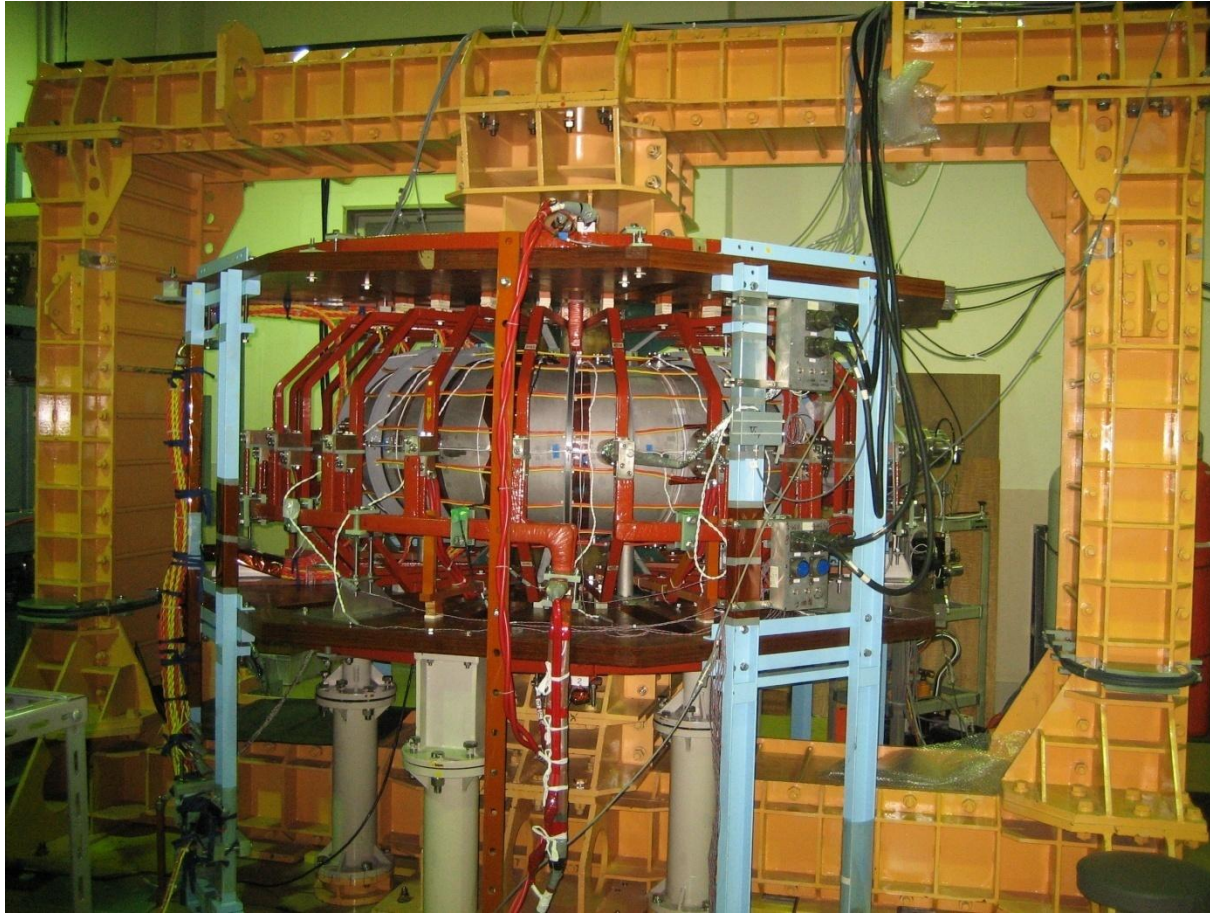
¹⁾*Hiroshima University, Higashi-hiroshima, Japan*

²⁾*Consorzio RFX, Padova, Italy*

³⁾*University of Tokyo, Kashiwa, Japan*

⁴⁾*National Institute for Advanced Industrial Science and Technology (AIST), Tsukuba, Japan*

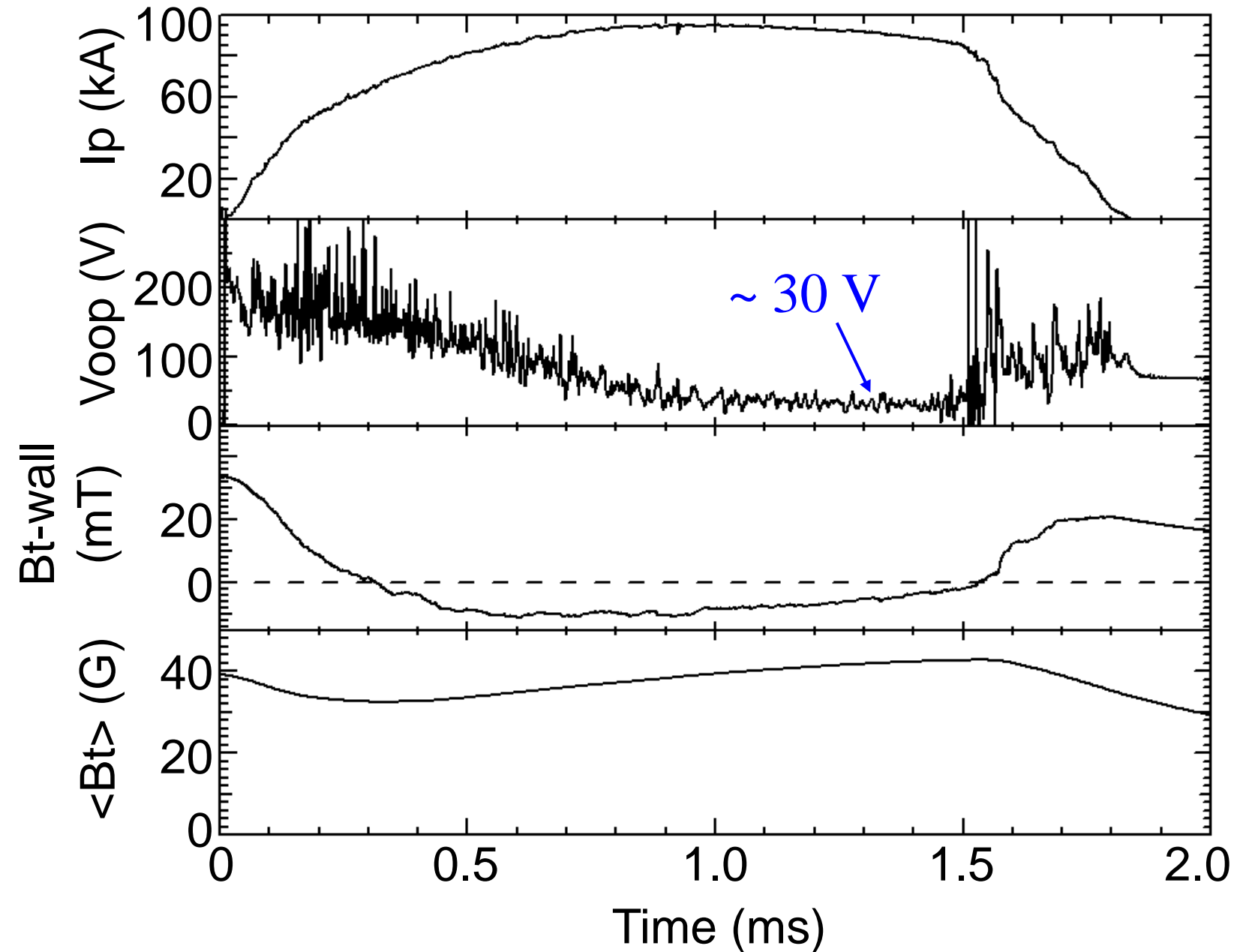
REversed field pinch of Low-Aspect-ratio eXperiment



- $R/a = A = 2$
(51 cm/25 cm)
- Optimization in progress

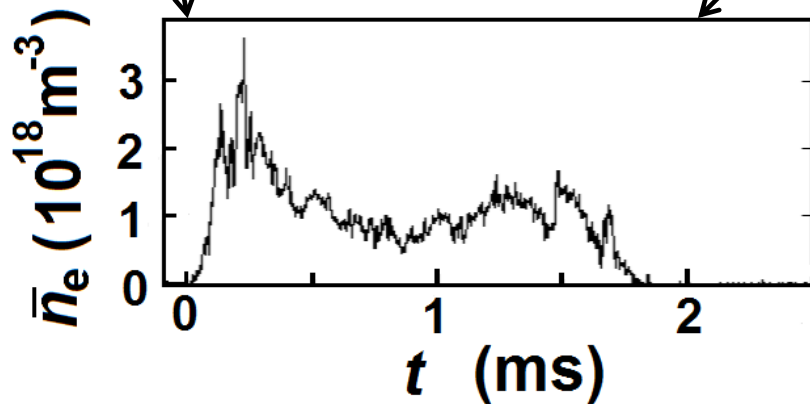
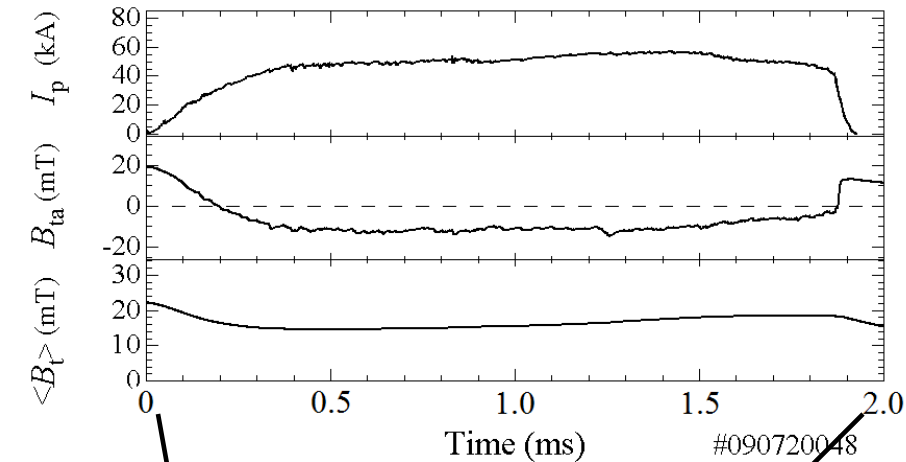
Kyoto Institute of Technology

Normal RFP discharges established

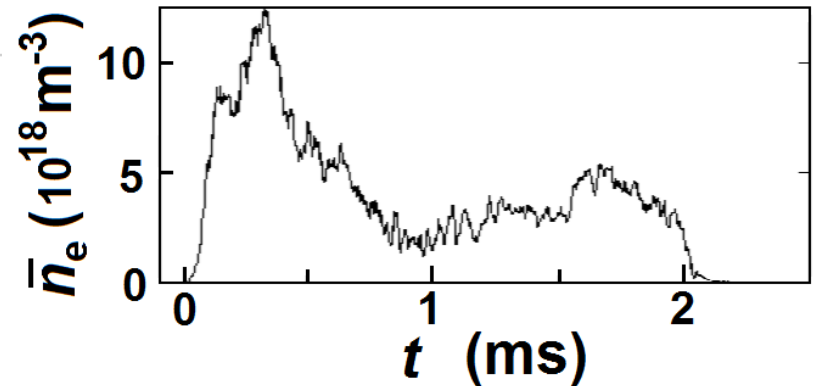
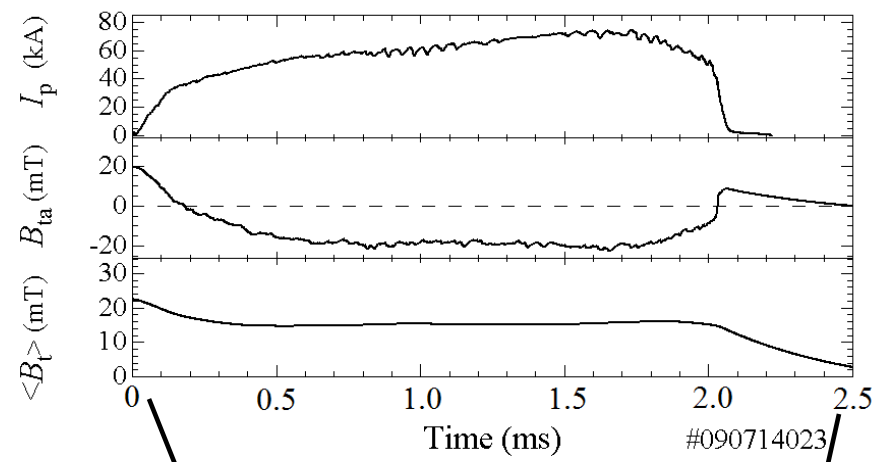


Density measurement with μ -wave interferometer

Density regime at flat-topped I_p phase: $1 - 10 \times 10^{18} \text{m}^{-3}$



low- n_e discharge

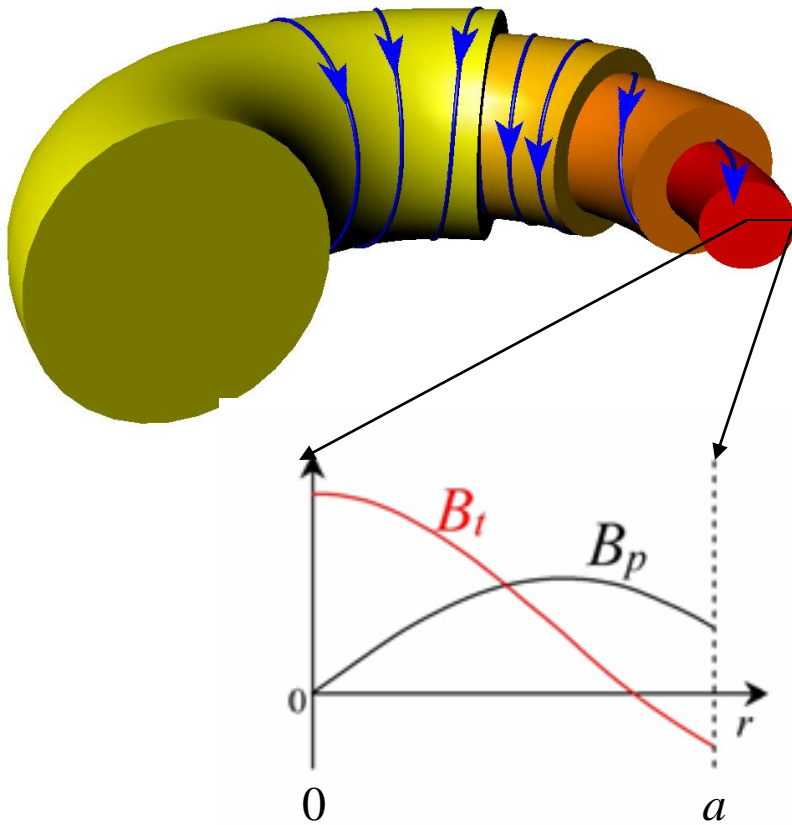


medium- n_e discharge

Outline

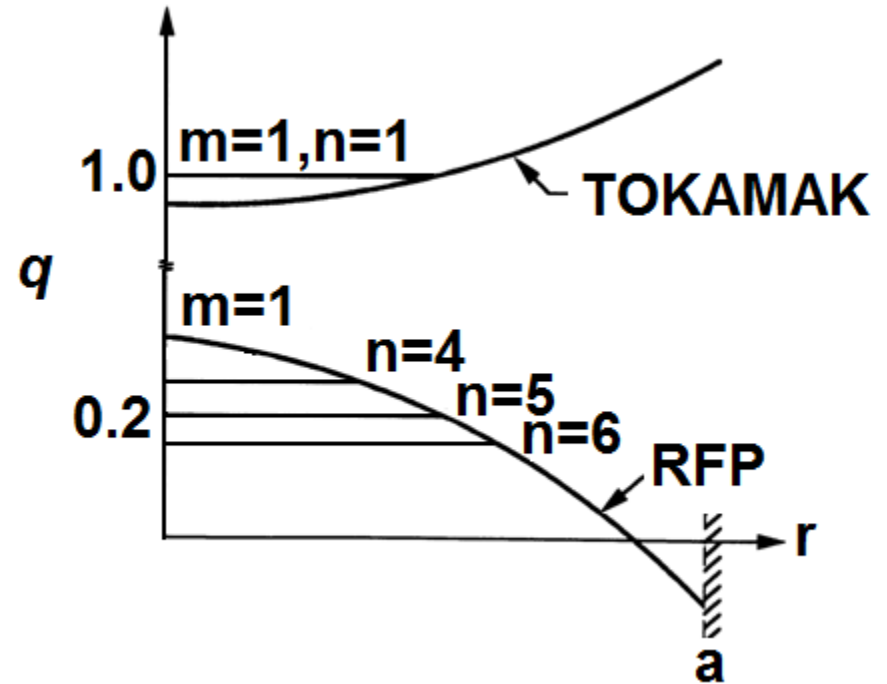
- Motivation to lowering A in the RFP
- Characterization of magnetic fluctuations in RELAX
- Helical structure in RELAX
- Magnetic structure and SXR emissivity in Helical Ohmic state
- Field line trace for RELAX plasmas
- Summary and future work

RFP configuration and its characteristics



$$B_{\text{toroidal}} \approx B_{\text{poloidal}}$$

$$q \ll 1$$



Peaked current profile

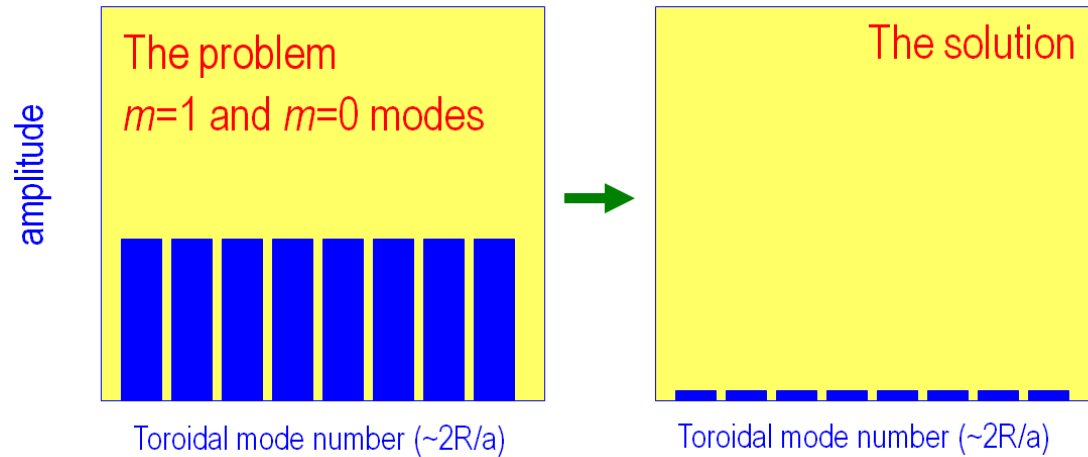
→ tearing mode unstable

Densely spaced mode rational surfaces

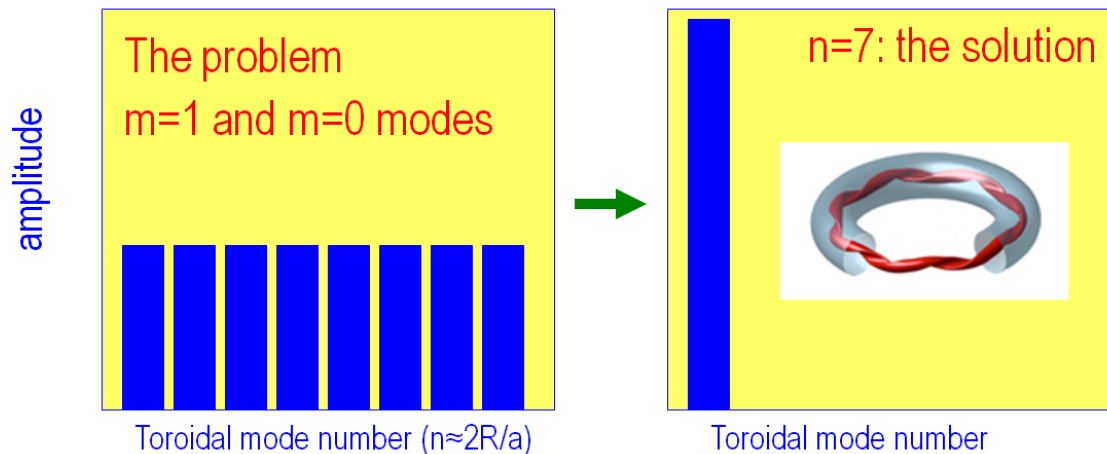
→ importance of nonlinear coupling

Two solutions to avoid magnetic chaos

(courtesy of P. Martin)

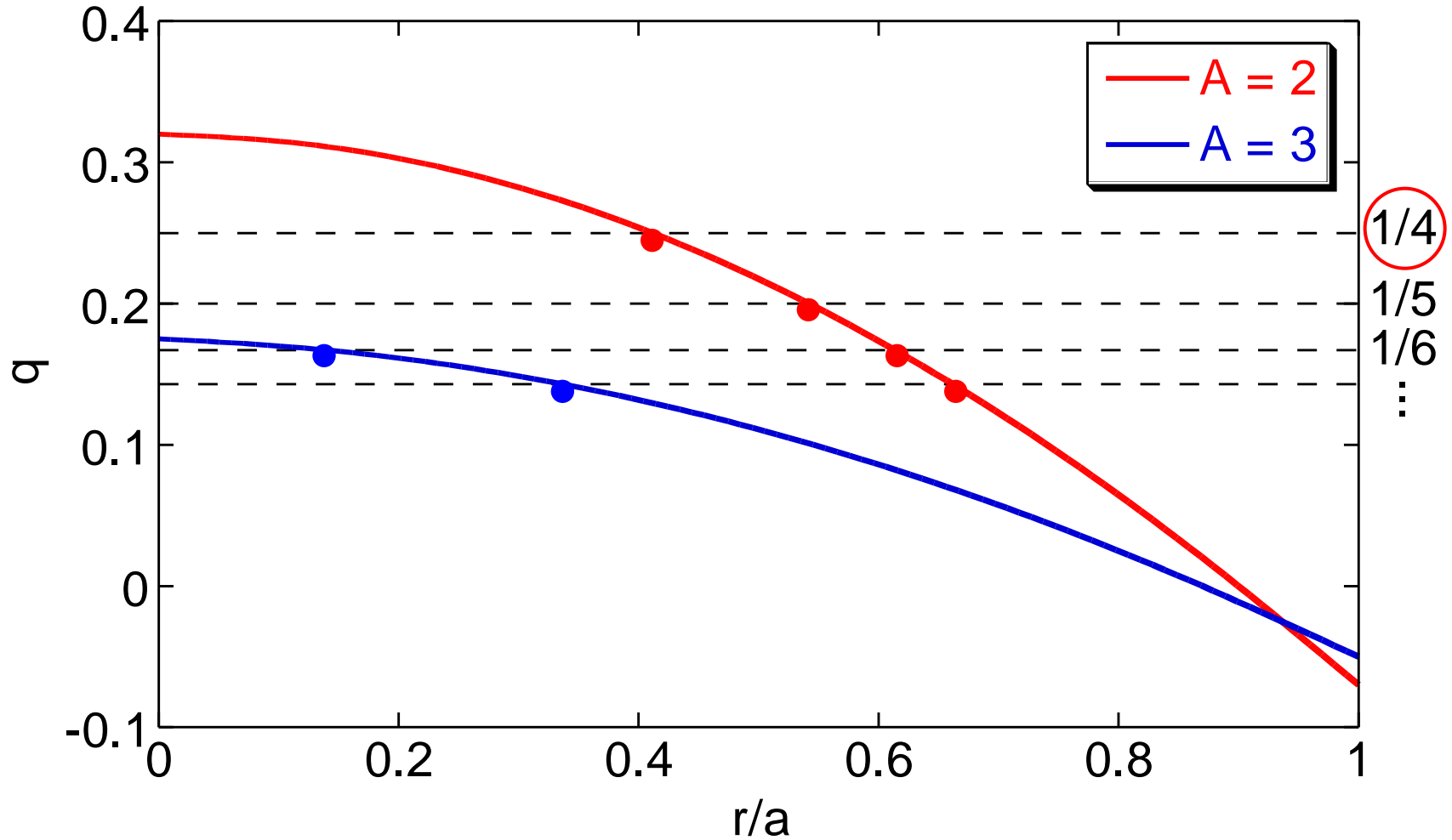


Suppression of all modes
 \Rightarrow PPCD in MST, etc



Concentration to single mode
 \Rightarrow QSH or SHAx in RFX, etc.

Lower A changes q profile - lower n of dominant $m=1$ modes



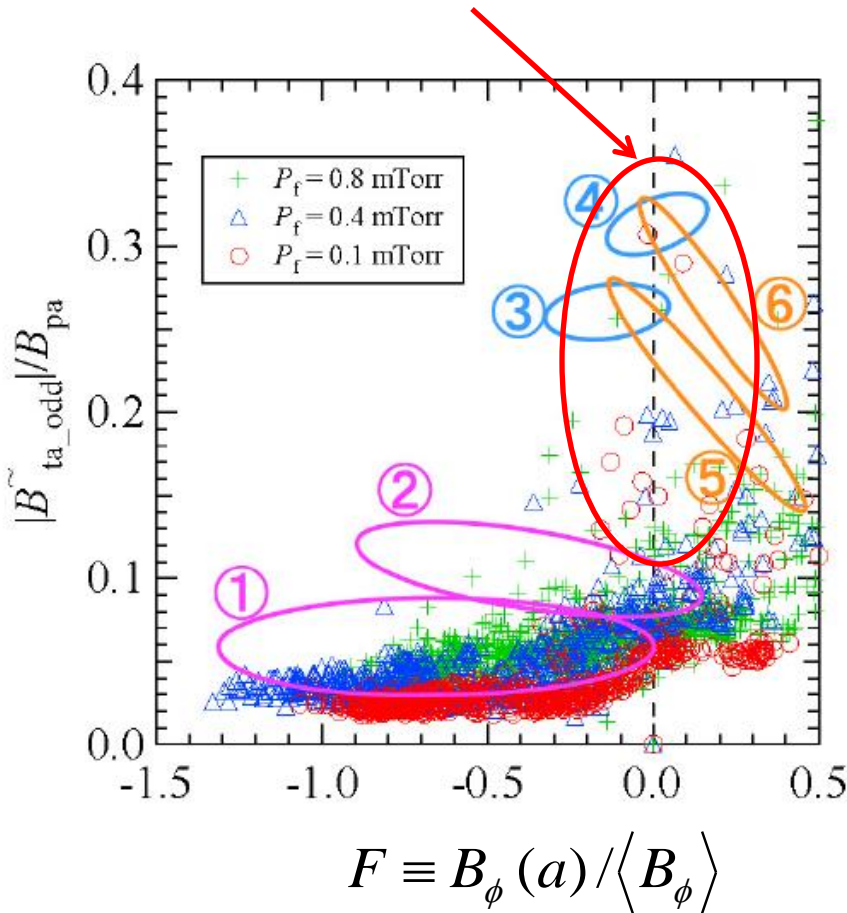
Goal of RELAX experiment

- Experimental study on advantages of low-A RFP configuration
 - Improved confinement with QSH for achieving high beta
 - Experimental identification of bootstrap current (target parameters:

$$T_e \sim 300 \text{eV}, n_e \sim 4 \times 10^{19} \text{m}^{-3} \text{ at } I_p \sim 100 \text{kA})$$

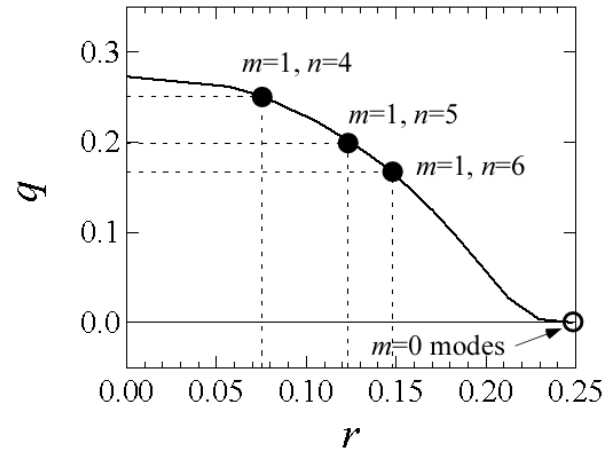
Magnetic fluctuation level depends on toroidal field reversal with transition to Helical Ohmic state at very shallow reversal

Transition to Helical state

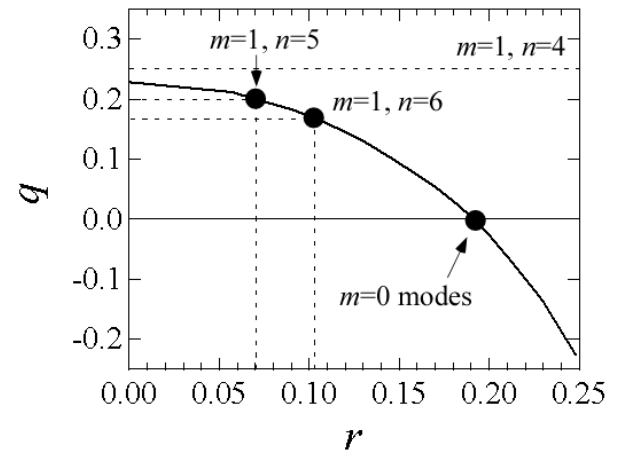


Fluctuation level of odd components

Comparison of q profiles



shallow reversal case



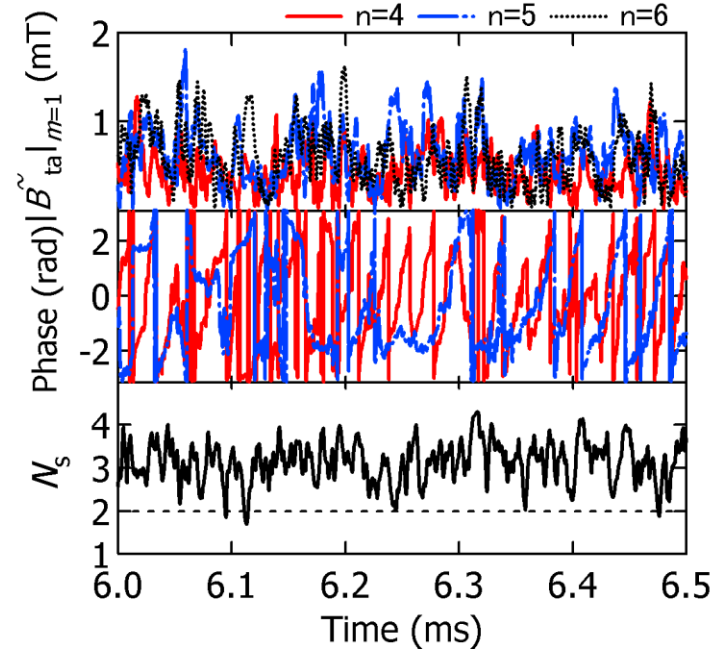
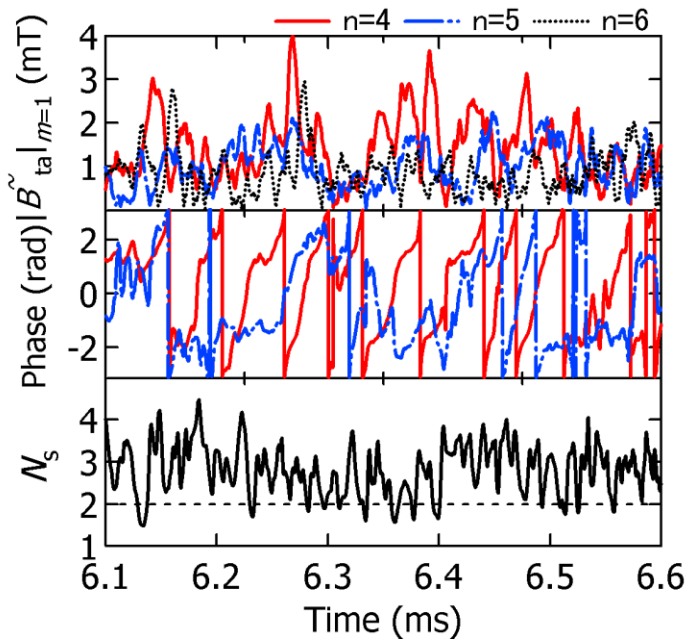
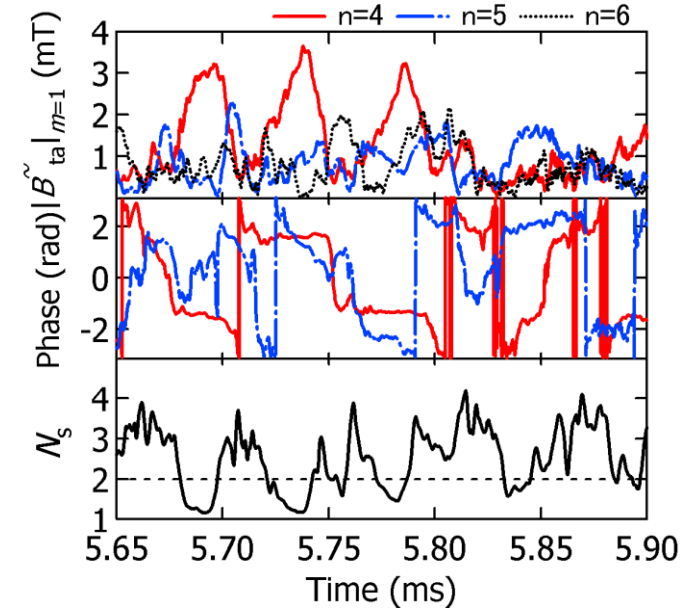
deep reversal case

Growth of dominant modes is related to mode rotation

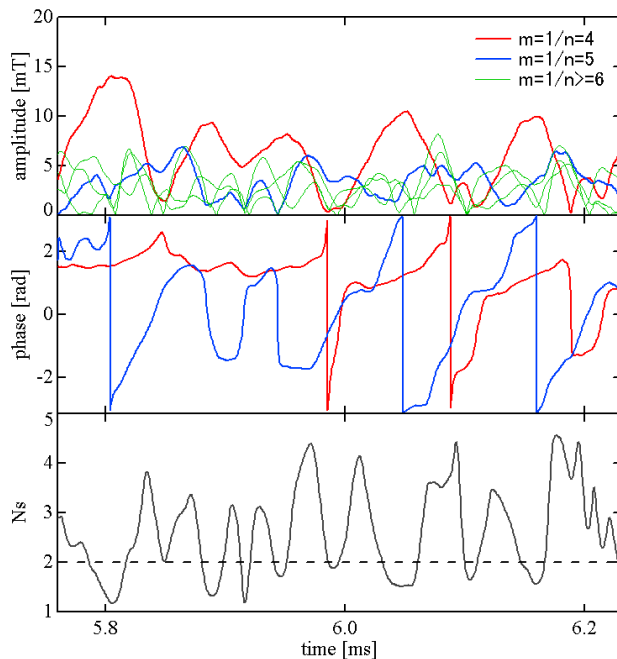
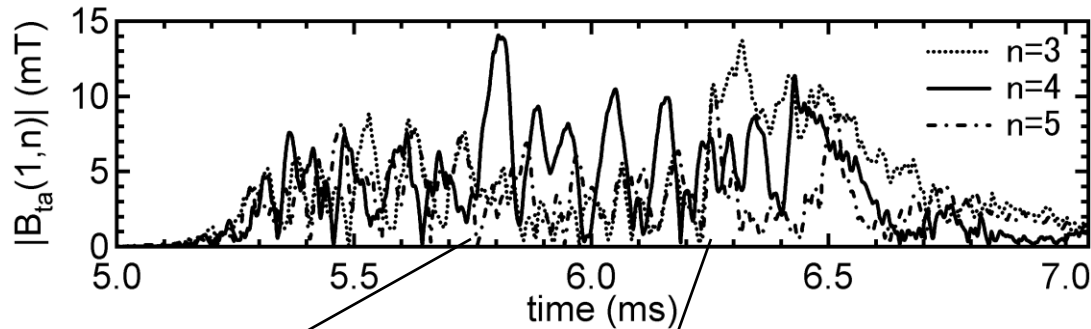
$m=1/n=4$ mode behavior:

- Longer QSH period for slower rotation
- Shorter QSH period with **higher spectral index N_s** for faster rotation

$$\text{Spectral index: } N_s = \left[\sum_{n=n_{\min}}^{n_{\max}} \left(\frac{b^2_{1,n}}{\sum_n b^2_{1,n}} \right)^2 \right]^{-1}$$

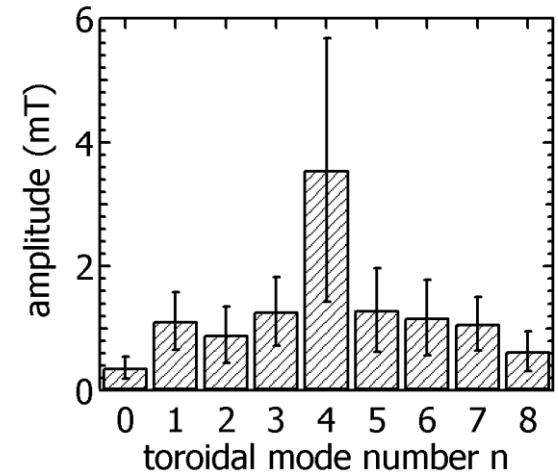


Quasi-periodic growth of a single dominant helical mode ($m=1/n=4$)



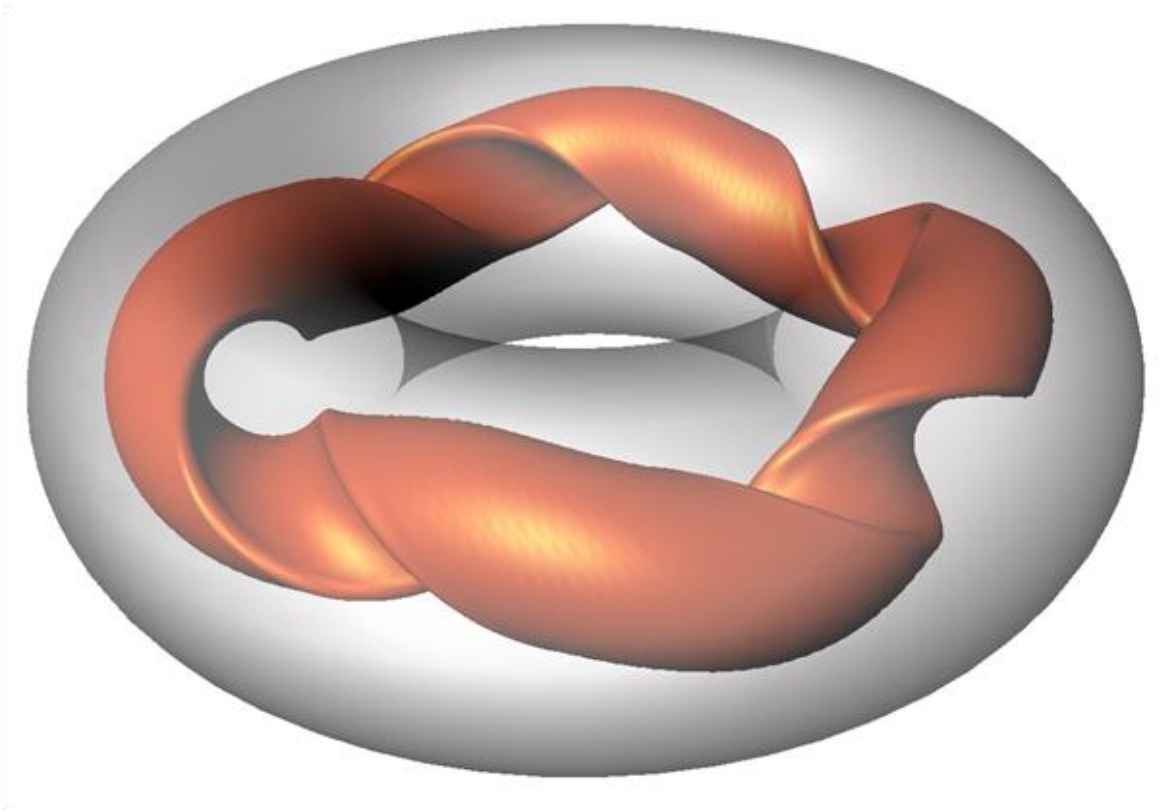
Spectral index N_s

$$N_s = \left[\sum_{n=n_{\min}}^{n_{\max}} \left(\frac{b_{1,n}^2}{\sum_n b_{1,n}^2} \right)^2 \right]^{-1}$$

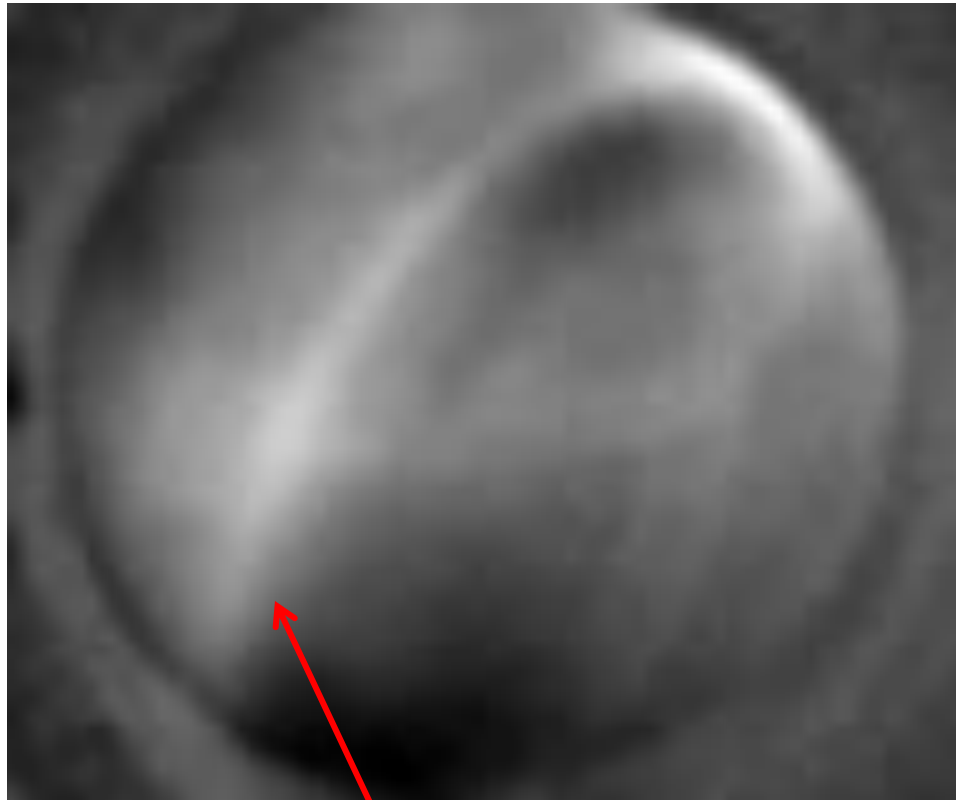


Characteristic of the QSH RFP state:
lower dominant mode number (mostly $n = 4$) and higher amplitudes than in other RFPs.

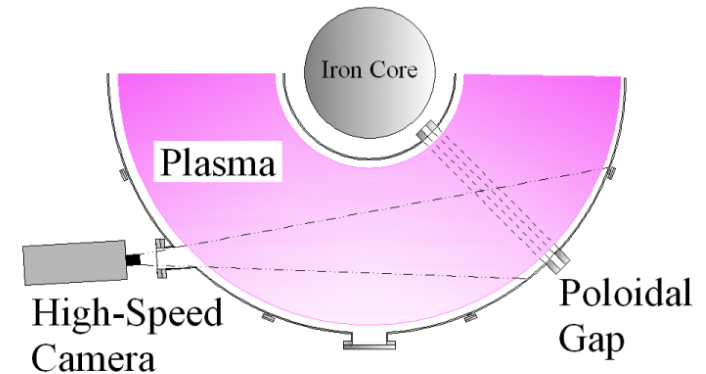
Magnetic island structure of QSH with $m=1/n=-4$



Rotating helical structure observed with high-speed camera - movie -



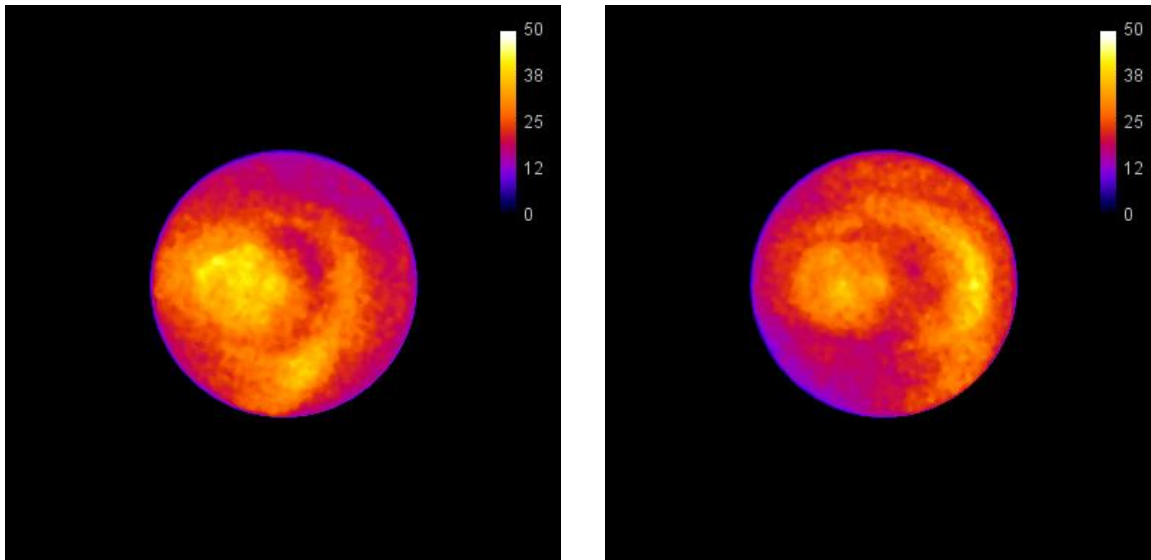
$m=1/n=-4$ helix



Tangential image:

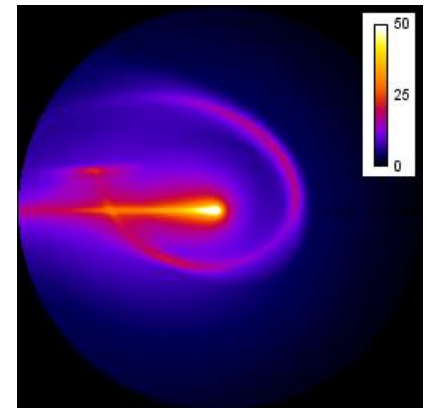
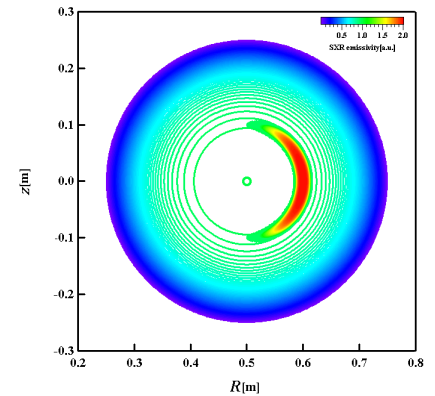
Following the initial bright phase, some structure starts to rotate, converging to a simple helix with $m/n=1/-4$.

Helical structure observed also in SXR pin-hole camera image



Pin-hole images with different phase

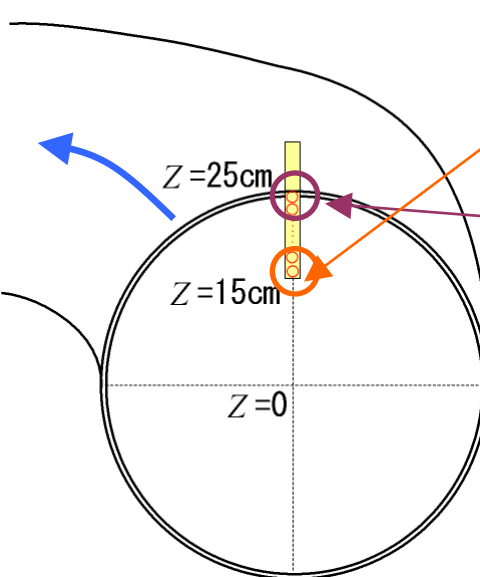
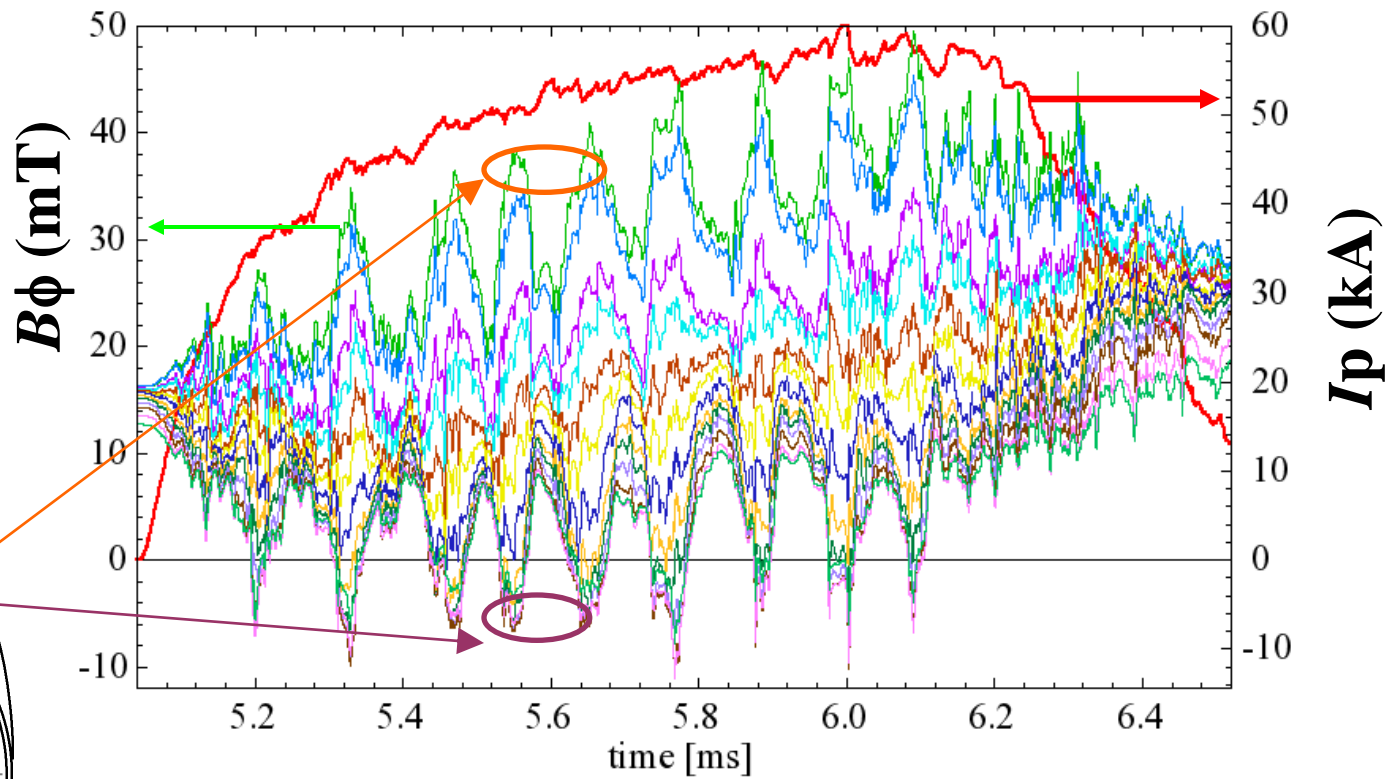
Exposure: $5\mu\text{s}$



Simulated image
with single island

Rotating Helical Ohmic Equilibrium state indicated - A large-scale magnetic field profile change -

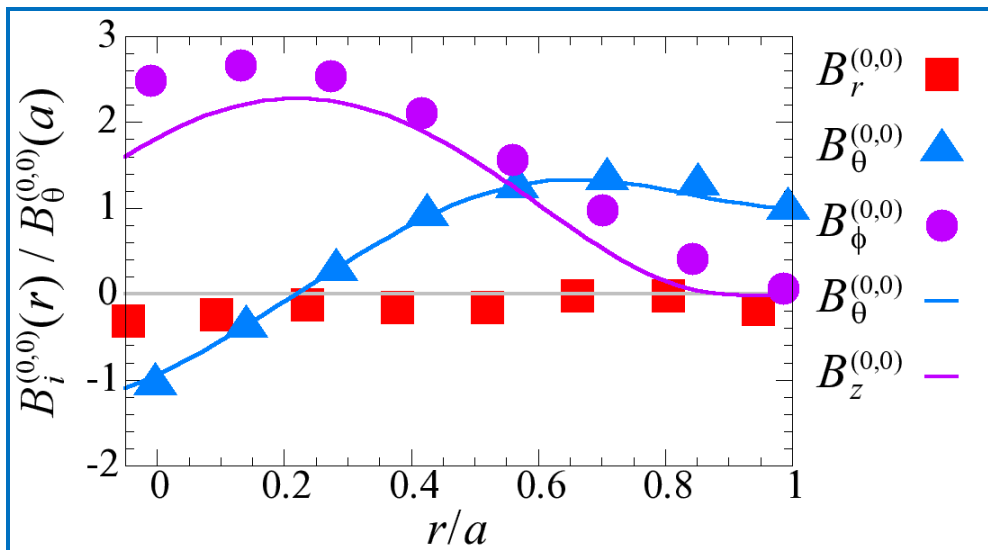
- Quasi-periodic oscillation between reversed and non-reversed profiles at a fixed point
- Similar large-scale oscillatory behavior in B_r and B_θ



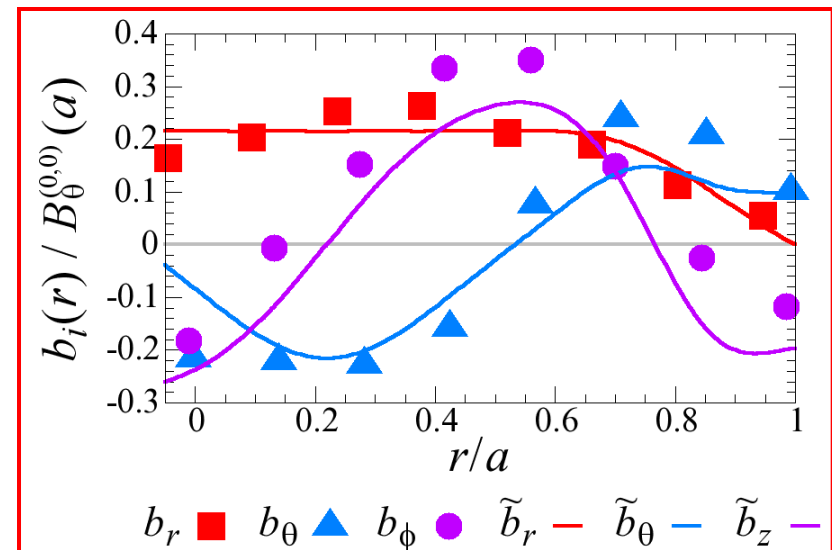
Plasma current	—	B_ϕ (Z=18.2cm)	—	B_ϕ (Z=21.4cm)	—	B_ϕ (Z=24.6cm)	—
B_ϕ (Z=15.8cm)	—	B_ϕ (Z=19.0cm)	—	B_ϕ (Z=22.2cm)	—	B_ϕ (Z=25.4cm)	—
B_ϕ (Z=16.6cm)	—	B_ϕ (Z=19.8cm)	—	B_ϕ (Z=23.0cm)	—		
B_ϕ (Z=17.4cm)	—	B_ϕ (Z=20.6cm)	—	B_ϕ (Z=23.8cm)	—		

Evidence of Helical Ohmic Equilibrium state

- **Symbols:** measured profiles with radial array of magnetic probes.
- **Solid lines:** Helical Ohmic equilibrium solution (Paccagnella (2000))
- Shafranov shift $\Delta/a \sim 0.2$.
- The helical structure rotates at a frequency of ~ 10 kHz.

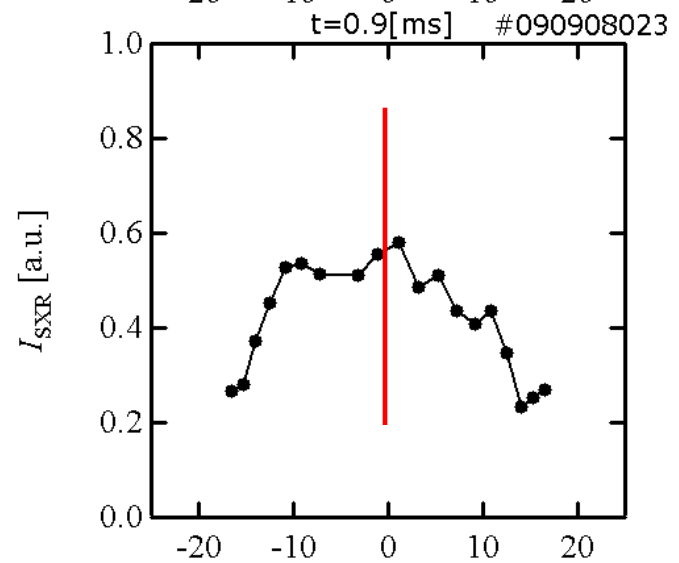
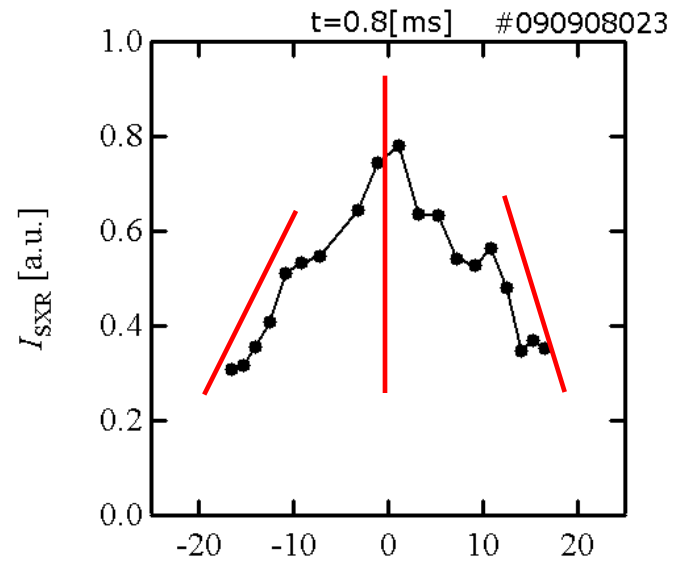
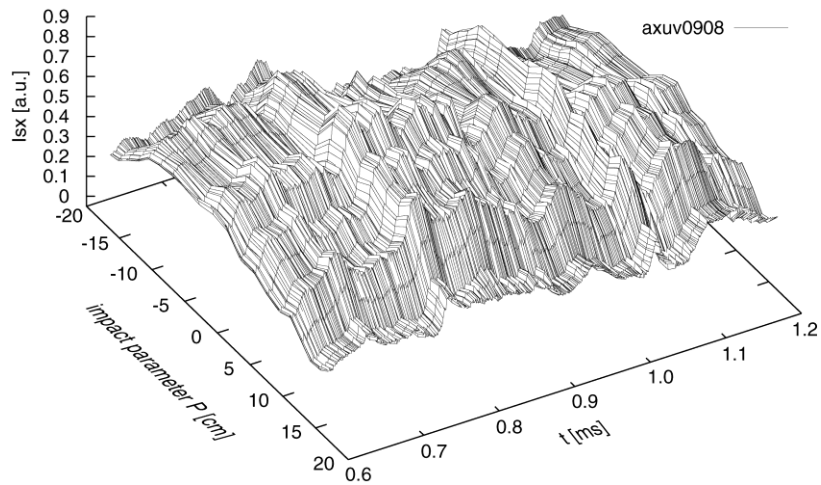
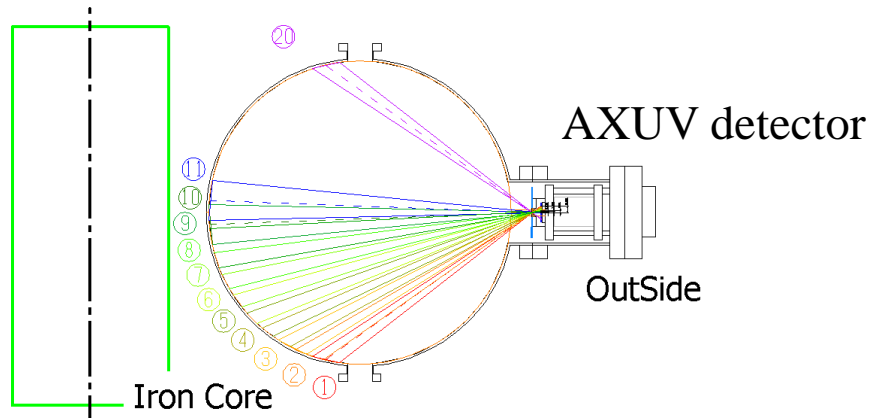


Axisymmetric components



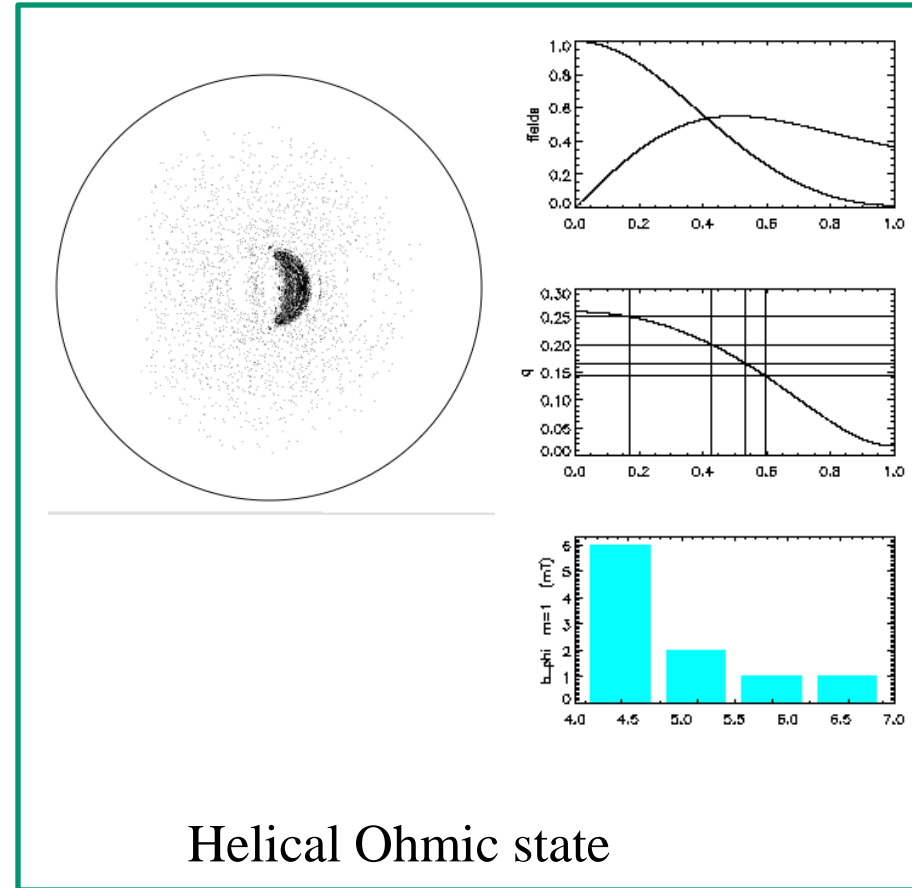
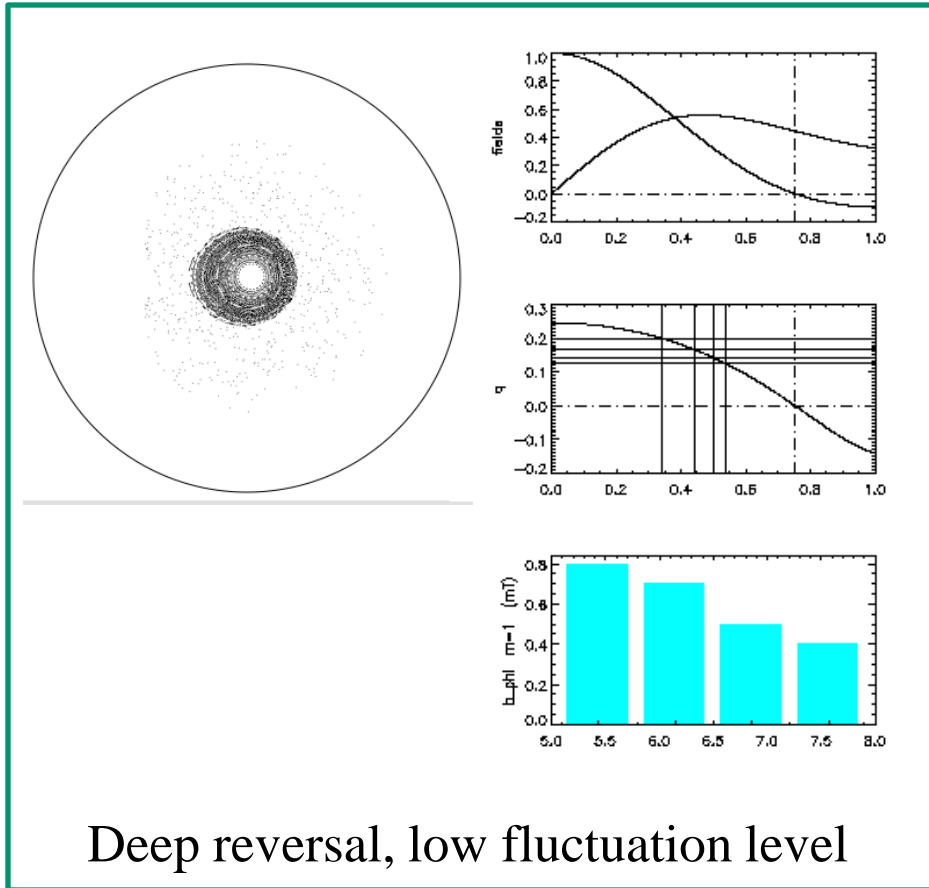
$m=1$ helical components

Evolution of asymmetric SXR emissivity profile



impact parameter (cm)

Field line trace with ORBIT code shows larger area of less stochastic region in deep-reversal case



1-D equilibrium, linear eigenfunction
in cylindrical geometry in ORBIT



**3-D equilibrium and 3-D
eigenfunctions are needed**

Summary

- RFP plasma with MHD properties characteristic to low- A configuration attained in RELAX
- Simple rotating helical structure observed
- Helical Ohmic Equilibrium state demonstrated
- 3-D equilibrium and stability analysis needed for further studies on magnetic structure of Helical Ohmic Equilibrium state

Future work

- Discharge performance improvement:
 - $I_p \sim 100\text{kA}$, $\tau \sim 3\text{ms} \Rightarrow 5\text{ms}$ (within present capability)
 - **Static helical perturbation and feedback control**

Further improvement of Helical Ohmic state will require improved magnetic boundary:

- **feedback control system**

Another means for confinement improvement (**current profile control**, e.g.) may be necessary

Helical Ohmic Equilibrium Solution

Grad-Shafranov equation with helical symmetry

$$\Delta_h \chi = \frac{1}{f} \frac{\partial}{\partial r} \left(f \frac{\partial \chi}{\partial r} \right) + \frac{1}{rf} \frac{\partial^2 \chi}{\partial u^2} = \left(c - \frac{dg}{d\chi} \right) g(\chi) - \frac{dp}{d\chi} (m^2 + k^2 r^2),$$

$$f = \frac{r}{m^2 + k^2 r^2}, \quad g = \frac{-2mk}{m^2 + k^2 r^2}$$

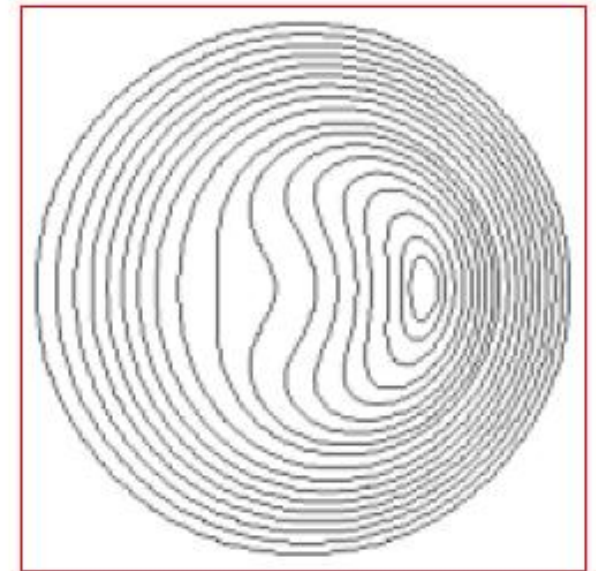
$$\lambda(r) = \frac{\mathbf{j} \cdot \mathbf{B}}{B^2} = \frac{dg}{d\chi} + \frac{g}{B^2} \frac{dp}{d\chi}$$

Ohm's law with helical symmetry

$$(\mathbf{E} + \mathbf{u} \times \mathbf{B} = \eta \mathbf{j})$$

$$E_0 \langle B_z \rangle_\chi = \eta(\chi) \left(\tilde{\lambda}(\chi) \langle B^2 \rangle_\chi + g \frac{dp}{d\chi} \right),$$

$$\hat{\lambda} = \frac{dg}{d\chi} = \frac{\mathbf{j} \cdot \mathbf{B}}{B^2} - \frac{g}{B^2} \frac{dp}{d\chi}$$



Contours of helical flux function

Theta=1.78, F=-0.06, beta=0.1